**DYNAMIC POSITIONING CONFERENCE**
**November 15-16, 2005**

## Operations II

---

# Watch Circle Assessment of Drilling Risers during a Drift-Off and Drive-Off Event of a Dynamically Positioned Vessel

Kenneth Bhalla and Yusong Cao

*Stress Engineering Services, Inc.*
*Houston, Texas. USA.*

---

Return to Session Directory

## ABSTRACT

The primary objective of a Drift-Off assessment is to address the behavior of a drilling riser when all thrusters lose power and are no longer capable of maintaining the drilling vessel on station. Whereas, the objective of the Drive-Off assessment is to assess the behavior of the drilling riser system when the thrusters malfunction and cause the drilling vessel to move away from station significantly. If any of these events occurs, an emergency disconnect must be initiated between the LMRP and BOP, otherwise a failure may occur in the riser or wellhead system.

The purpose of the Drift-Off and Drive-Off assessment is to determine green, yellow, and red watch circles of allowable vessel offset after which (Emergency Disconnect Sequence) EDS is initiated without damage to the riser. After the vessel exceeds the green watch circle, the vessel is in a degrading status. After the yellow watch circle is exceeded, preparations are made for EDS initiation. At the red alert, EDS is commenced.

The Drift-Off and Drive-Off response of a vessel is a function of the vessel characteristics and the environment. The vessel response and EDS allow operators to assess the risk associated with a given environment.

The Drive-Off and Drift-Off analysis starts with the effort to determine offset and heading as functions of time (trajectories) for the DP vessel in various Drive-Off and Drift-Off scenarios and environments.

Software and techniques have been developed to assist the DP vessel designer and operator to develop appropriate watch circles and assess the associated risk in a given environment. The in-house software DP-SHIPMO is used to determine the vessel Drift-Off and Drive-Off response. Commercial software ABAQUS and in-house software DERP are used to develop the riser response to the vessel Drift-Off and Drive-Off.

## 1.0 METHODOLOGY

The first phase of the process is to determine the vessel response trajectory as a function of time. The vessel trajectory consists of:

- Vessel offset as a function of time
- Vessel yaw as a function of time

The initial condition(s) of the vessel is critical in determining the vessel trajectory and consist of the following:

- Vessel heading
- Environment
- Wind/Wave direction
- Current direction
- Thruster schedule (how much thrust is applied, in what direction, and for how long)

Figure 1 shows an example of the vessel motion simulation to a Drive-Off event. The trajectory of the vessel is shown at equal time intervals. The thick red line shows the vessel position at the start of the event. The thin dark blue line indicates the position at which the riser would part. The simulation continues assuming the riser would not part. The post-failure simulation does not simulate the real situation but serves a means to verify the accuracy of the simulation. The black line indicates the "final" position of the vessel.

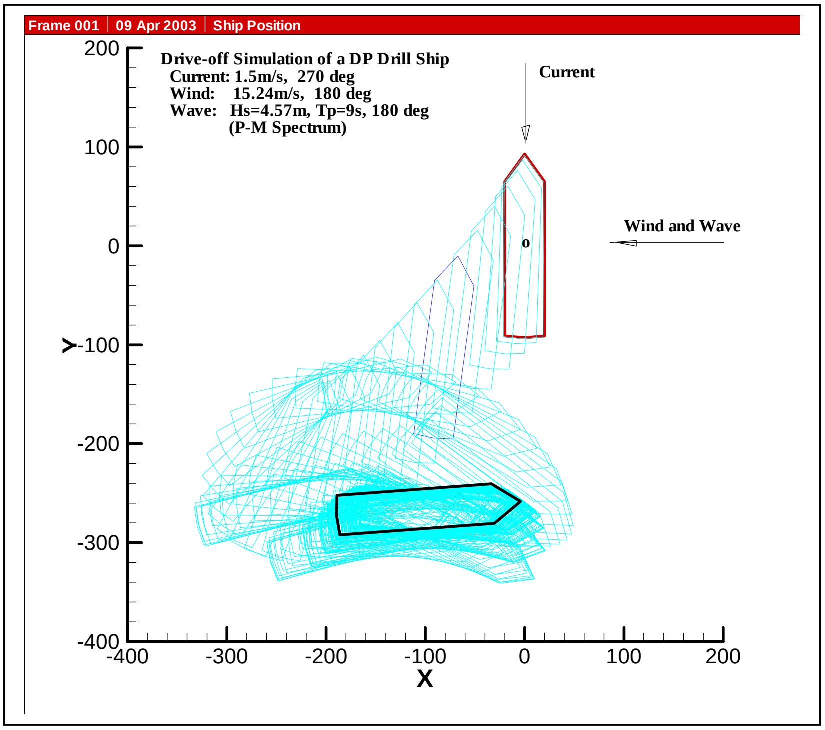

*Figure 1.1: Drive-Off Trajectory of a DP drillship vessel*

The trajectories are then supplied to a time domain finite element model of the riser, wellhead and casing system. The model consists of the following discrete components:

- upper flex joint
- riser tensioners (direct acting or wire-rope)
- telescopic joint (inner barrel and outer barrel)
- all riser joints
- lower flex joint
- BOP/LMRP
- wellhead connector
- high pressure wellhead housing
- structural conductor casing
- intermediate casings
- soil model

The results are post-processed to produce various responses as functions of time. Of interest will be the response of the following:

- tensioners stroke
- telescopic joint stroke
- upper flex joint angle
- lower flex joint angle
- maximum riser stress
- wellhead bending moment
- maximum stress in the structural conductor casing
- maximum stress in the intermediate casings
- unity check (per API RP 2A) in the conductor casing

The time-domain model does not explicitly include the dynamic response of the riser or vessel imposed by waves. Some of these responses will also have a significant wave-frequency component to them. For example, stroke will include a dynamic component caused by heave (which is a function of heading). This can be calculated separately. Likewise, the upper and lower flex joint angle will vary as a function of heading. These dynamic angles can be calculated from an in-house frequency domain riser model. These dynamic components will be included in the Drive-Off and Drift-Off analysis by superposing the dynamic component on the results from the time-domain model.

The results of the assessment provide a set of plots for each Drive-Off or Drift-Off scenario. The plots will show the response history of the riser/wellhead and casing system as functions of time with their allowable limits. The point at which the first limit is reached indicates the point of disconnect. Subtracting the associated time for the EDS, from the point of disconnect, will lead to the largest allowable radius for the red watch circle. In addition, subtracting off the time required to prepare for disconnect from the red watch circle provides the allowable yellow watch circle., A desirable result would be for the red and yellow watch circle to be much larger than the watch circle that the DP Vessel would normally operate within. If the results show watch circles that are too small or nonexistent, then the result is a limitation on the operating environment or some rethinking of the strategy for emergency disconnect criteria applied to the analysis would be required.

The following flowchart outlines the process used to determine the vessel watch circles and consider the feasibility of the environment and initial conditions to ensure that the integrity of the riser/wellhead/casing system is not compromised.

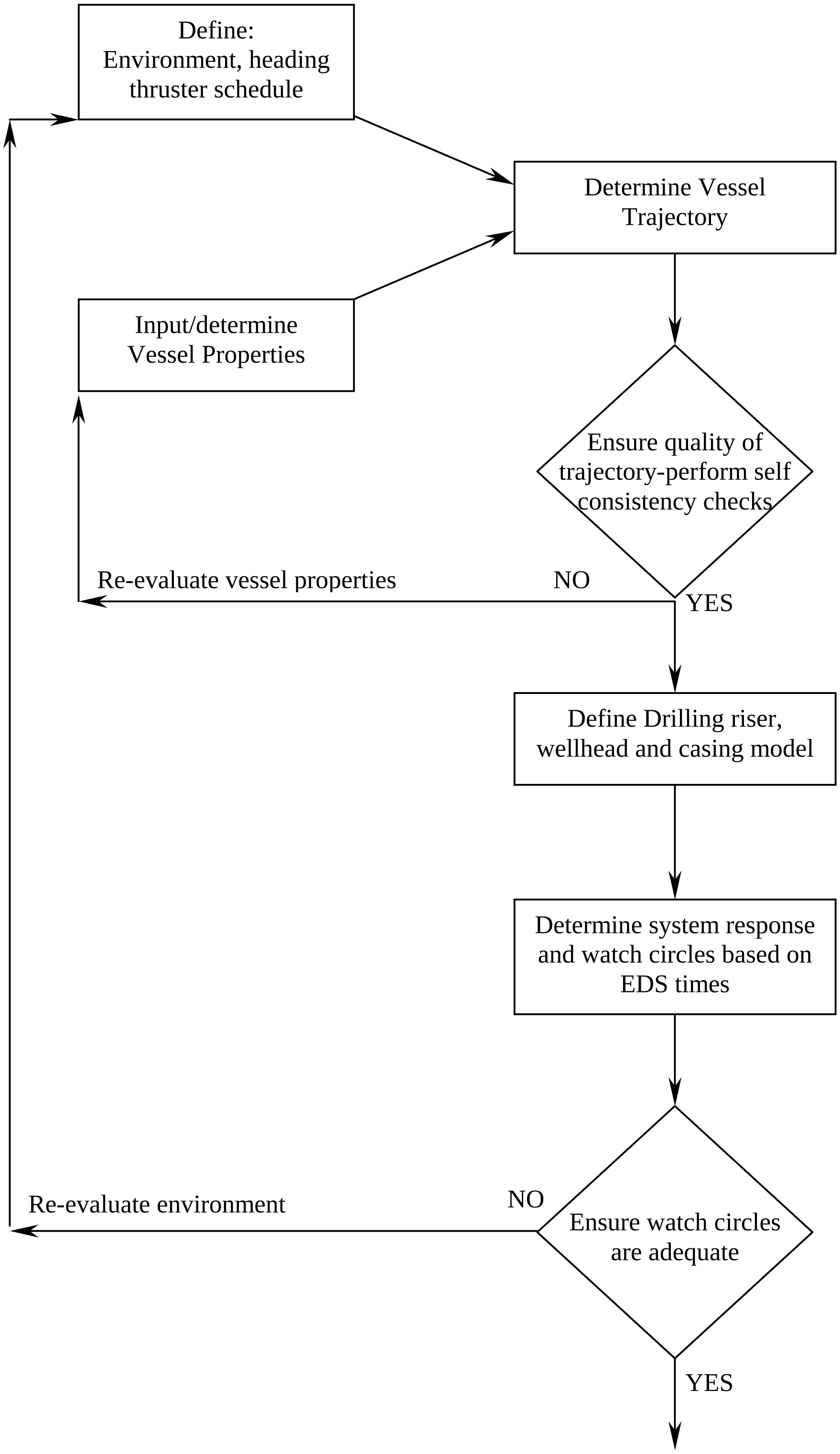

*Figure 1.2: Watch Circle Assessment Flow Chart*

## 2.0 VESSEL TRAJECTORY DETERMINATION

The motion of the vessel in the horizontal plane (surge, sway and yaw) is considered since the offset and yaw of the vessel from the well location needs to be determined. The heave, roll and pitch are not included in the vessel trajectory simulations. The effect of the wave induced heave, roll and pitch motions waves on the drilling riser are considered separately.

The vessel is modeled as a rigid body. Two coordinate systems are used to describe the motion of the vessel, a global coordinate system $O\,X\,Y$ and a moving coordinate system fixed to the vessel $O\,x_o y_o$ (Figure 2.1.1). The origin of the vessel-fixed coordinate system is at the vessel's center of gravity. The $O\,x_o$ axis is on the center plane of the vessel. The yaw (heading) angle is defined as the angle of the $O\,x_o$ axis measured from $O\,X$ axis (positive counter-clock wise).

### 2.1 Equations of motions

The dynamic equations for the plane motion of a rigid body is simply,

$$\begin{cases} M\ddot{X}_g = F_X \\ M\,\ddot{Y}_g = F_Y \\ I_z\,\ddot{\psi} = Q_Z \end{cases} \qquad (1)$$

where $M$ is the mass of the body, $I_Z$ is the moment of inertia of the body about the vertical axis through the center of gravity, ( $X_g, Y_g$ ) is the coordinate of the center of gravity in the global coordinate system. $F_X, F_Y$, and $Q_Z$ are the total forces and moment acting on the body. The double dots above a variable denote the second derivative with respect to time.

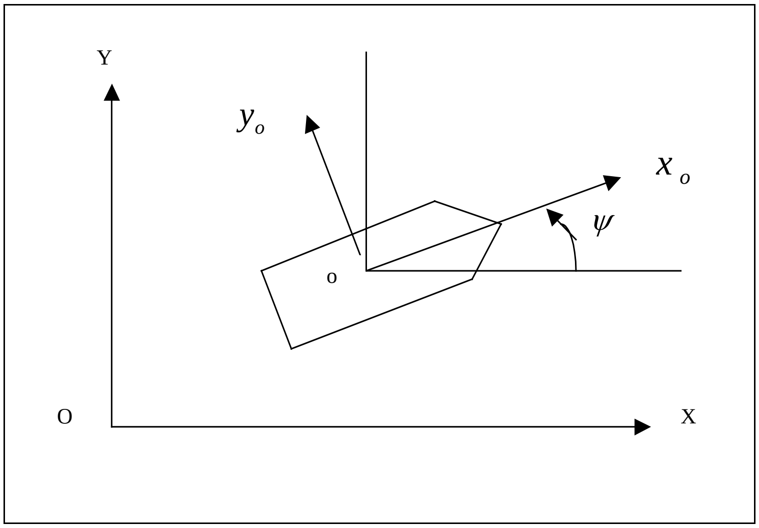

*Figure 2.1.1 Vessel Coordinate systems*

Let $(u, v)$ be the vessel velocity components in the vessel-fixed coordinate system, then we have,

$$\begin{cases} u = \dot{X}_g \cos\psi + \dot{Y}_g \sin\psi \\ v = -\dot{X}_g \sin\psi + \dot{Y}_g \cos\psi \end{cases} \tag{2}$$

or

$$\begin{cases} \dot{X}_g = u\cos\psi - v\sin\psi \\ \dot{Y}_g = u\sin\psi + v\cos\psi \end{cases} \tag{3}$$

where ( $\dot{X}_g, \dot{Y}_g$ ) are the vessel velocity components in the global coordinate system.

Let ( $F_{x_o}, F_{y_o}$ ) be the force components in the vessel-fixed coordinate system. Similarly, we have the following relation between ( $F_{x_o}, F_{y_o}$ ) and ( $F_X, F_Y,$ ),

$$\begin{cases} F_{x_o} = F_X \cos\psi + F_Y \sin\psi \\ F_{y_o} = -F_X \sin\psi + F_Y \cos\psi \end{cases} \tag{4}$$

or

$$\begin{cases} F_X = F_{x_o} \cos\psi - F_{y_o} \sin\psi \\ F_Y = F_{x_o} \sin\psi + F_{y_o} \cos\psi \end{cases} \tag{5}$$

Denote the yaw rate as,

$$r = \dot{\psi} \tag{6}$$

Differentiating Eq. (3) with respect to time, we have,

$$\begin{cases} \ddot{X}_g = \dot{u}\cos\psi - ur\sin\psi - \dot{v}\sin\psi - vr\cos\psi \\ \ddot{Y}_g = \dot{u}\sin\psi + ur\cos\psi + \dot{v}\cos\psi - vr\sin\psi \end{cases} \tag{7}$$

Substituting Eqs. (5) and (7) into Eq. (1), after manipulation, we obtain,

$$\begin{cases} M\,\dot{u} = M\,vr + F_{x_o} \\ M\,\dot{v} = -M\,ur + F_{y_o} \\ I_Z \dot{r} = Q_Z \end{cases} \tag{8}$$

Combining Eqs. (3), (6), and (8) gives,

$$\begin{cases} \dot{X}_g = u\cos\psi - v\sin\psi \\ \dot{Y}_g = u\sin\psi + v\cos\psi \\ \dot{\psi} = r \\ M\dot{u} = M\,vr + F_{x_o} \\ M\dot{v} = -M\,ur + F_{y_o} \\ I_Z \dot{r} = Q_z \end{cases} \tag{9}$$

The external force/moment acting on the vessel can be expressed as,

$$\begin{cases} F_{x_o} = F_{x_o}^{hydro} + F_{x_o}^{wind} + F_{x_o}^{thruster} + F_{x_o}^{riser} \\ F_{y_o} = F_{y_o}^{hydro} + F_{y_o}^{wind} + F_{y_o}^{thruster} + F_{y_o}^{riser} \\ Q_Z = Q_Z^{hydro} + Q_Z^{wind} + Q_Z^{thruster} + Q_Z^{riser} \end{cases} \tag{10}$$

The superscripts “hydro”, “wind”, “thruster”, and “riser” denote the force/moments due to hydrodynamic load, wind, thrusters and riser on the vessel, respectively.

The hydrodynamic load is further decomposed into,

$$\begin{cases} F_{x_o}^{hydro} = -A_{\dot u}^x \dot u - A_{\dot v}^x \dot v - A_{\dot r}^x \dot r + B_r^x r + \tilde F_{x_o}(\overline{U},\beta) + F_{x_o}^{drift} \\ F_{y_o}^{hydro} = -A_{\dot u}^y \dot u - A_{\dot v}^y \dot v - A_{\dot r}^y \dot r + B_r^y r + \tilde F_{y_o}(\overline{U},\beta) + F_{y_o}^{drift} \\ Q_Z^{hydro} = -A_{\dot u}^z \dot u - A_{\dot v}^z \dot v - A_{\dot r}^z \dot r + B_r^z r + \tilde Q_z(\overline{U},\beta) + Q_z^{drift} \end{cases} \tag{11}$$

On the right-hand-side of each of the above three equations, the first three terms are due to the acceleration of the vessel, the fourth term due to the rotational velocity of the vessel, the fifth term due to the relative flow velocity (magnitude $\overline{U}$ and heading $\beta$) to the vessel, and the last term due to the wave drift. Eq. (11) can be rewritten in matrix form,

$$\begin{pmatrix} F_{x_o}^{hydro} \\ F_{y_o}^{hydro} \\ Q_z^{hydro} \end{pmatrix} = -\begin{pmatrix} A_{\dot u}^x & A_{\dot v}^x & A_{\dot r}^x \\ A_{\dot u}^y & A_{\dot v}^y & A_{\dot r}^y \\ A_{\dot u}^z & A_{\dot v}^z & A_{\dot r}^z \end{pmatrix} \begin{pmatrix} \dot u \\ \dot v \\ \dot r \end{pmatrix} + \begin{pmatrix} B_r^x \\ B_r^y \\ B_r^z \end{pmatrix} r + \begin{pmatrix} \tilde F_{x_o}(\overline{U},\beta) + F_{x_o}^{drift} \\ \tilde F_{y_o}(\overline{U},\beta) + F_{y_o}^{drift} \\ \tilde Q_z(\overline{U},\beta) + Q_z^{drift} \end{pmatrix} \tag{12}$$

The square matrix in Eq. (12) is referred to as the added mass matrix **A**. Combining Eqs. (9), (10) and (12), we have the following equation in matrix form,

$$\mathbf{M}\dot{\mathbf{X}} = \mathbf{B} \tag{13}$$

where,

$$\mathbf{M} = \begin{pmatrix} 1 & 0 & 0 & 0 & 0 & 0 \\ 0 & 1 & 0 & 0 & 0 & 0 \\ 0 & 0 & 1 & 0 & 0 & 0 \\ 0 & 0 & 0 & M + A_{\dot u}^x & A_{\dot v}^x & A_{\dot r}^x \\ 0 & 0 & 0 & A_{\dot u}^y & M + A_{\dot v}^y & A_{\dot r}^y \\ 0 & 0 & 0 & A_{\dot u}^z & A_{\dot v}^z & I_Z + A_{\dot r}^z \end{pmatrix} \tag{14}$$

$$\mathbf{X} = \begin{pmatrix} X_g \\ Y_g \\ \psi \\ u \\ v \\ r \end{pmatrix} \quad \text{and} \quad \dot{\mathbf{X}} = \begin{pmatrix} \dot{X}_g \\ \dot{Y}_g \\ \dot{\psi} \\ \dot{u} \\ \dot{v} \\ \dot{r} \end{pmatrix} \tag{15}$$

and

$$\mathbf{B} = \begin{pmatrix} u\cos\psi - v\sin\psi \\ u\sin\psi + v\cos\psi \\ r \\ B_r^x\, r + \tilde{F}_{x_o}(\overline{U},\beta) + F_{x_o}^{drift} + F_{x_o}^{wind} + F_{x_o}^{thrust} + F_{x_o}^{riser} \\ B_r^y\, r + \tilde{F}_{y_o}(\overline{U},\beta) + F_{y_o}^{drift} + F_{y_o}^{wind} + F_{y_o}^{thrust} + F_{y_o}^{riser} \\ B_r^z\, r + \tilde{Q}_z(\overline{U},\beta) + Q_z^{drift} + Q_z^{wind} + Q_z^{thrust} + Q_z^{riser} \end{pmatrix} \tag{16}$$

The hydrodynamic derivatives, i.e. ( $B_r^x, B_r^y, B_r^z$ ) and the added mass matrix **A**, are the vessel's hydrodynamic characteristics and only depend on the vessel geometry and the water density. The inversion of Eq. (13) is,

$$\dot{\mathbf{X}} = \mathbf{M}^{-1}\mathbf{B} \tag{17}$$

Eq. (17) is a system of ordinary differential equations about the state variable vector **X** with respect to time, provided the added mass matrix **A**, ( $B_r^x, B_r^y, B_r^z$ ), **B** are known. Several standard numerical ODE solvers are available for solving Eq. (17) for **X**. The Fehlberg fourth-fifth order Runge-Kutta method which is very stable and accurate is chosen.

## 2.2 Force/Moment Calculations

### *2.2.1 Force/moment due to the relative flow velocity to the vessel*

Usually, the forces and moment of this nature are assumed to be quadratic functions of the relative velocity $\overline{U}$ and are expressed as,

$$\begin{cases} \tilde{F}_{x_o}(\overline{U},\beta) = C_{x_o}^c(\beta)\,\overline{U}^2 \\ \tilde{F}_{y_o}(\overline{U},\beta) = C_{y_o}^c(\beta)\,\overline{U}^2 \\ \tilde{Q}_z(\overline{U},\beta) = C_z^c(\beta)\,\overline{U}^2 \end{cases} \tag{18}$$

They have the same form as those of force/moment due to a current on the stationary vessel. The hydrodynamic coefficients, $C_{x_o}^c(\beta)$ , $C_{y_o}^c(\beta)$ and $C_z^c(\beta)$ are referred to as the current force/moment coefficients and can be determined by the model tests. The current direction $\beta$ is defined in the vessel-fixed coordinate system, measured from the axis.

### *2.2.2 Mean force/moment due to wave drift*

The mean wave drift forces and moment vary with the wave direction $\beta_{wave}$ relative to the vessel. They can be calculated using (Faltinsen, 1990),

$$\begin{cases} F_{x_o}^{drift}(\beta_{wave}) = 2\int_0^{\infty} S(\omega)\, C_{x_o}^{drift}(\omega;\beta_{wave})\, d\omega \\ F_{y_o}^{drift}(\beta_{wave}) = 2\int_0^{\infty} S(\omega)\, C_{y_o}^{drift}(\omega;\beta_{wave})\, d\omega \\ Q_{z}^{drift}(\beta_{wave}) = 2\int_0^{\infty} S(\omega)\, C_{z}^{drift}(\omega;\beta_{wave})\, d\omega \end{cases} \tag{19}$$

where $\beta_{wave}$ is the wave direction measured in the vessel-fixed coordinate system. $C_{x_o}^{drift}(\omega;\beta_{wave})$, $C_{y_o}^{drift}(\omega;\beta_{wave})$, and $C_{z}^{drift}(\omega;\beta_{wave})$ are the quadratic drift force/moment transfer functions. They can be calculated using WAMIT. $S(\omega)$ is the wave spectrum for a given environment.

### *2.2.3 Force/moment due to the wind*

Similar to the force and moment relationships due to the flow velocity of the vessel, the forces and moment on the exposed part of the vessel from wind loading are assumed to have the same form of quadratic functions of the relative wind velocity $\overline{U}_{wind}$,

$$\begin{cases} F_{x_o}^{wind}(\overline{U}_{wind},\beta_{wind}) = C_{x_o}^{wind}(\beta_{wind})\,\overline{U}_{wind}^{2} \\ F_{y_o}^{wind}(\overline{U}_{wind},\beta_{wind}) = C_{y_o}^{wind}(\beta_{wind})\,\overline{U}_{wind}^{2} \\ Q_{z}^{wind}(\overline{U}_{wind},\beta_{wind}) = C_{z}^{wind}(\beta_{wind})\,\overline{U}_{wind}^{2} \end{cases} \tag{20}$$

where $\beta_{wind}$ is the wind direction measured in the vessel-fixed coordinate system. $C_{x_o}^{wind}(\beta_{wind})$, $C_{y_o}^{wind}(\beta_{wind})$, and $C_{z}^{wind}(\beta_{wind})$ are the wind force/moment coefficients.

### *2.2.4 Force/moment due to the thrusters*

Each thruster is assumed to provide a concentrated thrust force at the point the thruster is located and in the direction of the thruster's azimuthing (measured in the vessel-fixed coordinate system). Since the thruster is usually not located at the vessel's center of gravity, it also provides a moment on the vessel. Let $T_i$ be the thrust from the i$^{th}$ thruster, then the total forces and moment provided by all the N thrusters are,

$$\begin{cases} F_{x_o}^{thruster} = \sum_{i=1}^{N} T_i \cos\beta_i^{thrust} \\ F_{y_o}^{thruster} = \sum_{i=1}^{N} T_i \sin\beta_i^{thrust} \\ Q_{Z}^{thruster} = \sum_{i=1}^{N} \left[ -(T_i\cos\beta_i^{thrust})\,\hat{x}_i + (T_i\sin\beta_i^{thrust})\,\hat{y}_i \right] \end{cases} \tag{21}$$

where $\beta_i^{thrust}$ is the azimuth angle of the i$^{th}$ thruster. $(\hat{x}_i, \hat{y}_i)$ is the location of the i$^{th}$ thruster in the vessel-fixed coordinate system.

Thrust $T_i$ is assumed to be the only functions of the propeller $RPM_i$ and the relative velocity of the flow entering the thruster (in the opposite direction of the thruster azimuth angle), $V_i^a$ (also referred to as the advance velocity),

$$T_i = f_T(RPM_i, V_i^a) \qquad (22)$$

All the thrusters on a vessel may typically have the same function $f_T(RPM, V^a)$, which is graphically presented in Figure 2.2.4.1. Given the propeller RPM and the advance velocity as a function of time, the thrust can be determined by interpolation from the thrust~RPM curves in the figure.

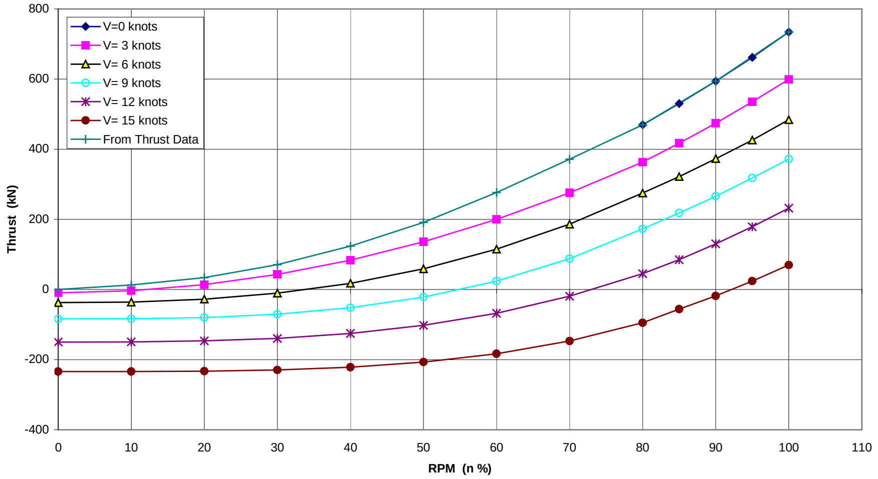

*Figure 2.2.4.1 Thrust vs. RPM curves for different advance velocities.*

### *2.2.5 Force/moment due to the drilling riser*

The drilling riser provides a restoring force/moment to the vessel. For small vessel offset (<15% of the riser length), the effect of the riser on the vessel is model as a spring with a stiffness of,

$$K_r = \frac{T_r}{L_r} \tag{23}$$

where $T_r$ and $L_r$ are the riser's top tension and the length, respectively. It is also reasonable to assume that the changes in $T_r$ and $L_r$ are small when the vessel's offset is small, and therefore remain constant. The force and moment on the vessel due to the riser are then,

$$\begin{cases} F_{x_o}^{riser} = (-K_r(x_r - x_{ro}))\cos\psi + (-K_r(y_r - y_{ro}))\sin\psi \\ F_{y_o}^{riser} = -(-K_r(x_r - x_{ro}))\sin\psi + (-K_r(y_r - y_{ro}))\cos\psi \\ Q_Z^{riser} = F_{y_o}^{riser} D_{r-cg} \end{cases} \tag{24}$$

where $(x_r, y_r)$ is the location of the riser top to the vessel. $(x_{ro}, y_{ro})$ is the location of the wellhead. $(x_r, y_r)$ and $(x_{ro}, y_{ro})$ are measured in the global coordinate system. $D_{r-cg}$ is the horizontal distance of the riser top from the vessel's center of gravity. It is assumed that both the riser top attachment point and the vessel's center of gravity are in the center plane of the vessel.

It should be pointed out that the forces and moments from vessel movement, current, wind, wave, and thrusters are expressed in the vessel-fixed coordinate system. Because of the vessel movement, the relative flow velocity and direction to the vessel, the relative wave and wind directions, the forces and moments due to the current, wave drift and wind are time dependent. In addition, because of changes in the propeller RPM and the azimuth angle and the vessel movement, the forces and moments by the thrusters are also time dependent. A computer code **DP-SHIPMO** has been developed to solve the time dependent equations of motion and perform Drift-Off and Drive-Off simulations.

## 2.3 Hydrodynamic Derivatives

The hydrodynamic derivatives, the added mass matrix **A** and $(B_r^x, B_r^y, B_r^z)$, need to be determined before Eq. (17) can be solved. Sometimes, because of insufficient data, some approximations are made. A good understanding of the physical meanings of these derivatives is very helpful in making reasonable approximations.

Added mass matrix **A** :

$A_{\dot{u}}^x$ -- hydrodynamic reaction force on the vessel in the surge ($x_o$ axis direction) due to a unit acceleration of the vessel in surge. The effect of this force is usually significant.

$A_{\dot{v}}^x$ -- hydrodynamic reaction force on the vessel in the surge ($x_o$ axis direction) due to a unit acceleration of the vessel in sway ($y_o$ axis direction). If the vessel hull is fore-aft symmetric, this force should be zero. For slightly force-aft asymmetric hull, this force should be relatively small and may be neglected.

$A_r^x$ -- hydrodynamic reaction force on the vessel in the surge ( $x_o$ axis direction) due to a unit yaw acceleration of the vessel (about the vertical axis). If the vessel hull is fore-aft symmetric, this force should be zero. For slightly force-aft asymmetric hull, this force should also be relatively small and may be neglected.

$A_u^y$ -- hydrodynamic reaction force on the vessel in the sway ( $y_o$ axis direction) due to a unit acceleration of the vessel in surge ( $x_o$ axis direction). If the vessel hull is fore-aft symmetric, this force should be zero. For slightly force-aft asymmetric hull, this force should be relatively small and may be neglected.

$A_v^y$ -- hydrodynamic reaction force on the vessel in the sway ( $y_o$ axis direction) due to a unit acceleration of the vessel in sway ( $y_o$ axis direction). The effect of this force is usually very significant.

$A_r^y$ -- hydrodynamic reaction force on the vessel in the surge ( $y_o$ axis direction) due to a unit yaw acceleration of the vessel (about the vertical axis). If the vessel hull is fore-aft symmetric, this force should be zero. For slightly force-aft asymmetric hull, this force should also be relatively small and may be neglected.

$A_u^z$ -- hydrodynamic reaction moment on the vessel about the z axis due to a unit acceleration of the vessel in surge ( $x_o$ axis direction). If the vessel hull is fore-aft symmetric, this moment should be zero. For slightly force-aft asymmetric hull, this force should be relatively small and may be neglected.

$A_v^z$ -- hydrodynamic reaction moment on the vessel about the z axis due to a unit acceleration of the vessel in sway ( $y_o$ axis direction). For a vessel with port-starboard symmetry which is the case for most vessels, this moment is zero. We assume the port-starboard symmetry. Therefore, this term vanishes.

$A_r^z$ -- hydrodynamic reaction moment on the vessel about the z axis due to a unit yaw acceleration of the vessel (about the vertical axis). The effect of this force is usually very significant.

Hydrodynamic derivatives ( $B_r^x, B_r^y, B_r^z$ ):

$B_r^x$ --hydrodynamic reaction force on the vessel in surge due to a unit yaw rotational velocity (yaw rate). If the vessel hull is fore-aft symmetric, this force should be zero. For slightly force-aft asymmetric hull, this force should also be relatively small and may be neglected.

$B_r^y$ --hydrodynamic reaction force on the vessel in sway due to a unit yaw rotational velocity (yaw rate). If the vessel hull is fore-aft symmetric, this force should be zero. For slightly force-aft asymmetric hull, this force should also be relatively small and may be neglected.

$B_r^z$ --hydrodynamic reaction moment on the vessel due to a unit yaw rotational velocity (yaw rate). The effect of this force is usually very significant.

In one case that was considered $A_{\dot{u}}^{x}$, $A_{\dot{v}}^{y}$ and $A_{\dot{r}}^{z}$ was furnished. The hull of vessel consisted of a large portion of parallel mid-section, it can be considered as only slightly fore-aft asymmetric. The remaining derivatives in $\mathbf{A}$, $B_r^x$ and $B_r^y$ were approximated as zero, based on the understanding of their physical significance. $B_r^z$ was the remaining derivative that was significant and can not be neglected, but not readily available.

In this case, $B_r^z$ was collaborated and determined indirectly by comparing the vessel trajectory of a turning circle test using the numerical simulation with the measured trajectory in the sea trial. In the collaboration, an initial guess of $B_r^z$ was made, then the same sea trial event was simulated with the same vessel's initial speed, control schedules of the thrusters' RPM and azimuth angles used in the sea trial. The numerically simulated trajectory was compared to the measured one. $B_r^z$ was adjusted based on the comparison and another simulation was performed and comparison made. The process repeated until the numerical simulation compared reasonably well with the sea trial measurement (visual graphical judgment). Figure 2.3.1 shows the comparison of the numerical simulation with the sea trial data using an adjusted $B_r^z$.

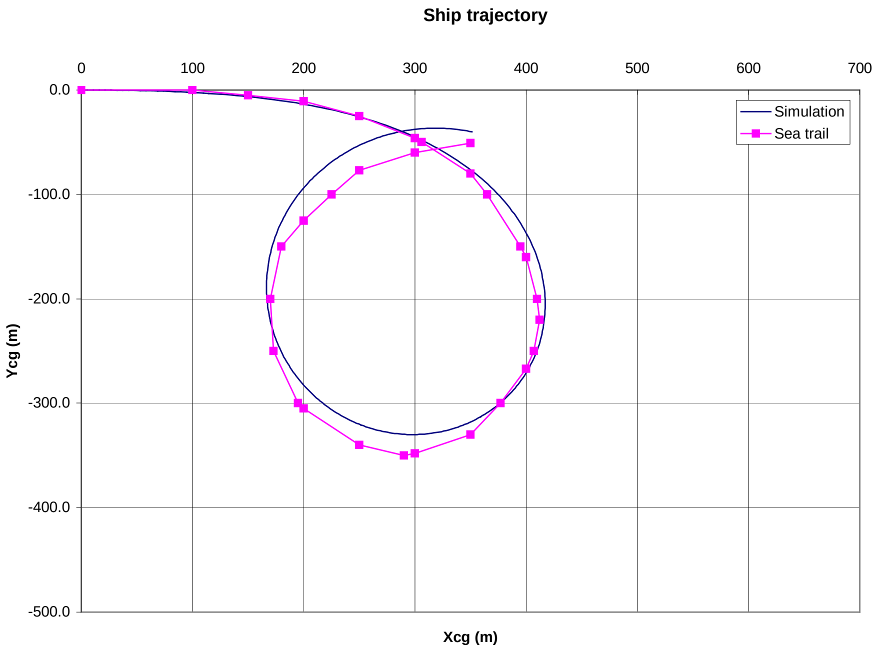

*Figure 2.3.1 Comparison of the simulated vessel trajectory with a sea trial measurement*

The comparison showed in Figure 2.3.1 was deemed acceptable since a "perfect" match was considered impossible and unnecessary to attempt because of the uncertainty in the actual environmental conditions during the sea trial and error in the measurement. The environment was certainly not perfectly calm during the sea trial, while the numerical simulation assumed no wind, current and waves.

The agreement between the numerical result and the measured data is also a very good indication that the approximations for the other hydrodynamic derivatives were adequate. It was believed that if one of the derivatives had been wrong, it would have been unlikely that a good agreement between the numerical simulation and the sea trial data could be achieved by simply adjusting $B_r^z$.

The quality of the hydrodynamic model for the vessel was further assured with some self-consistency tests. These may include, but are not limited to:

*Symmetry tests*:
For instance, the vessel turns to starboard when the two aft thrusters azimuth to the port side with remaining thrusters pointing ahead. The vessel should turn to the port side if the aft thrusters azimuth to the starboard with the same angle, and the vessel's trajectory should be a perfect image of the former case about the vessel's center plane.

*Turning circle tests*:
Considering the same example in the symmetry test, the larger the thruster's azimuth angle, the sharper the vessel should turn and the smaller the diameter of the turning circle of the trajectory should be.

*Crash Stop astern tests*:
In a crash stop astern test, the vessel is initially traveling along a straight line at a constant speed with all the thrusters running at some RPM and pointing straight ahead. Given the stop command, all the thrusters turn 180 degrees and run at the full design RPM to stop the vessel. The higher the initial speed, the longer it takes to bring the vessel to the full stop and the longer the vessel travels before the stop.

*Effect of Environment*
The vessel should turn and drift to starboard side if the wind (current or waves) comes from the bow at a certain angle (< 90 degrees) on port side. Similarly, the vessel should turn and drift to port side if the environment comes on starboard side.

The numerical tests qualitatively confirmed the correct performance of the simulations. Therefore, the hydrodynamic model can be used, with a high degree of confidence, for simulations and analyses of Drive-Off and Drift-Off events.

## 2.4 Example Case

The following show examples of time history output (vessel position and yaw) from the DP-SHIPMO program:

Figure 2.4.1 shows the history of the vessel position plotted every 10 seconds. In this case, the vessel initially heads in the x axis. The current comes from the port side ($270^0$) and the wind and waves come from the bow at an angle on the port side ($195^0$). As seen, the vessel is drifts and its position is determined by the environmental forces after the thrusters lost the power (RPM=0). The position marked in red is the point in time when the offset of the riser top attachment point has reached a given vessel offset.

The vessel position marked in black appears to show a static equilibrium at this position due to the environmental forces and riser restoring force/moment.

Figure 2.4.2 shows the trajectory of the vessel's CG and Figure 2.4.3 shows the coordinates, as well as the offset, of the vessel's CG as functions of time. Figure 2.4.4 shows the vessel's yaw angle as a function of time. As seen in Figure 2.4.4 and Figure 2.4.5, the CG and the yaw angle are approaching to a constant value, indicating a static equilibrium position.

The coordinates and offset of the riser top attachment point are shown in Figure 2.4.6. Figure 2.4.7 shows the riser offset for the first 300 seconds. From Figure 2.4.7, one can determine how much time it takes before the riser attains a given offset.

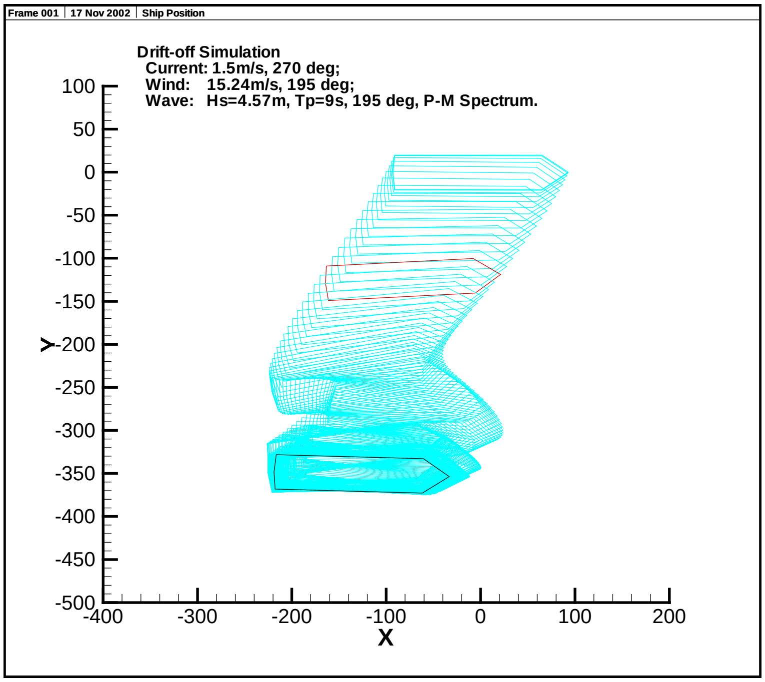

*Figure 2.3.2 History of the vessel position*

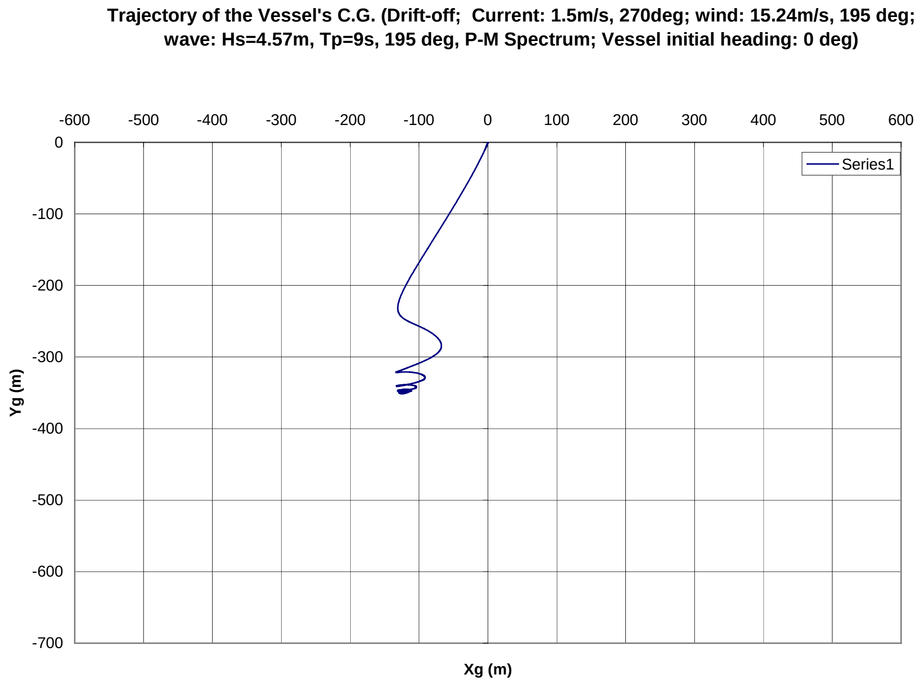

*Figure 2.3.3 Trajectory of vessel CG*

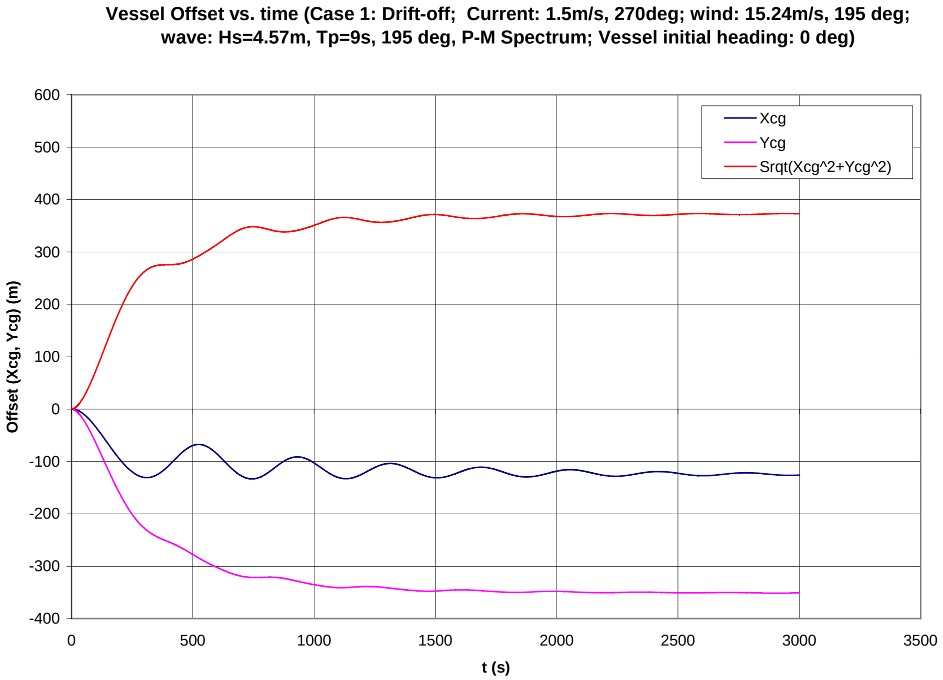

*Figure 2.3.4 Vessel CG X and Y Coordinates*

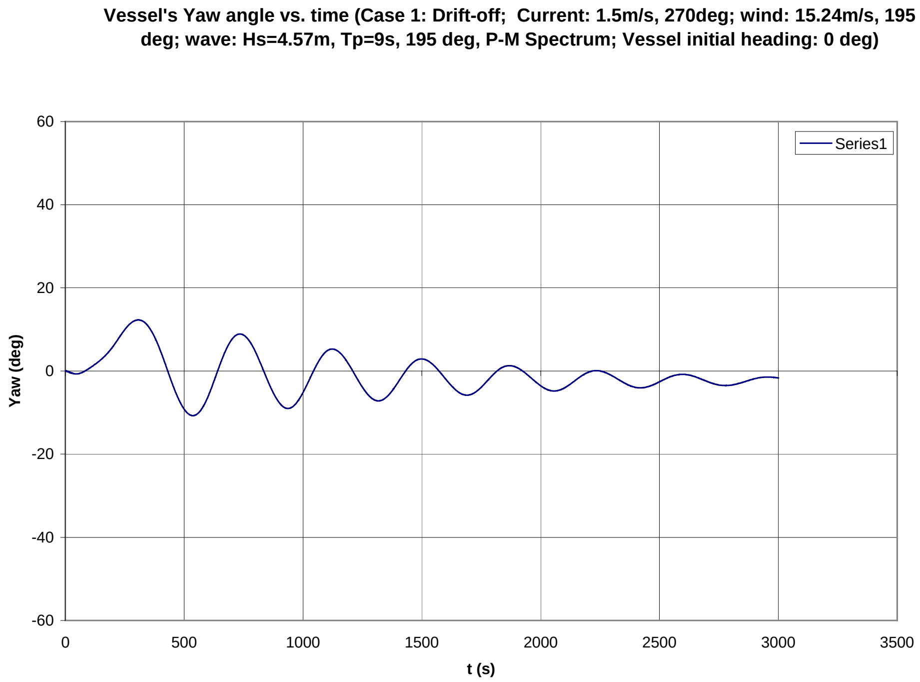

*Figure 2.3.5 Vessel yaw angle*

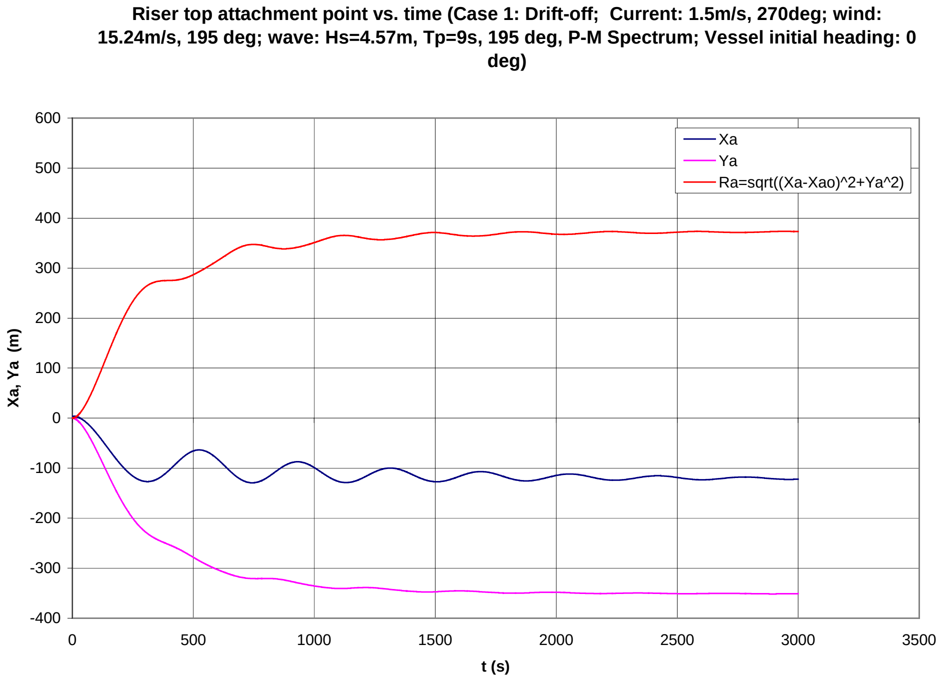

*Figure 2.3.6 Coordinates and offset of riser top attachment point*

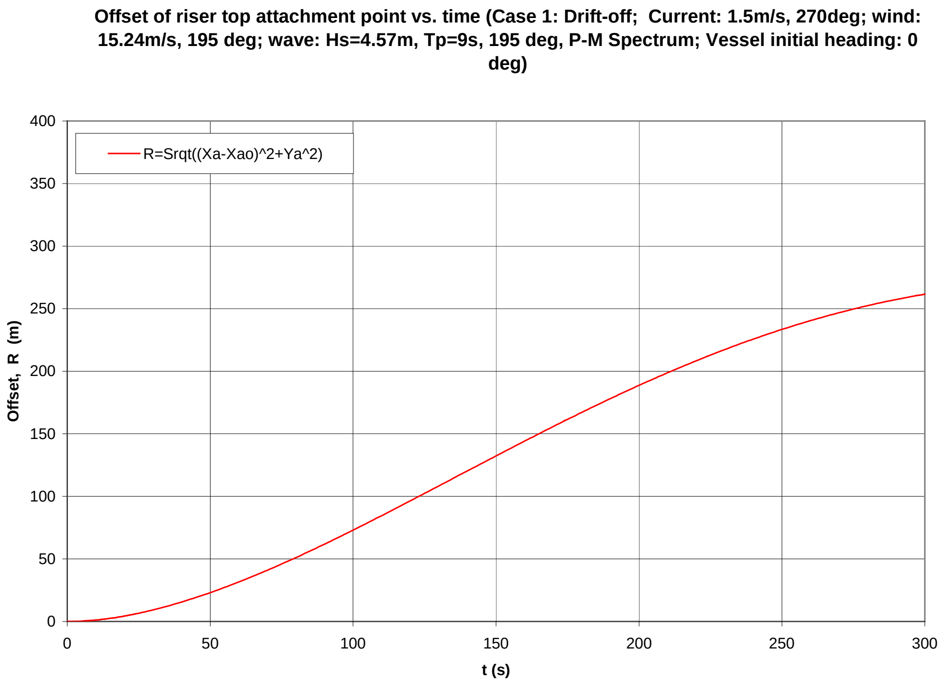

*Figure 2.3.7 Riser offset (Case 1)*

*(Same as in Figure 2.3.6 - plotted for the first 300 seconds)*

## 3.0 WATCH CIRCLE DETERMINATION

The purpose of the Drift-Off and Drive-Off analysis is to determine green, yellow and red watch circles of allowable vessel offset after which (Emergency Disconnect Sequence) EDS is initiated without damage to the riser, wellhead and the structural conductor casing. After the vessel exceeds the green watch circle, the vessel is in a degrading status. After the yellow watch circle is exceeded, preparations are made for EDS initiation. At the red alert, EDS is commenced.

Riser disconnect in a Drift-Off or Drive-Off scenario must occur before any of the following criteria is reached:

- Flex joint angles must be less than their allowable maxima
- Stroke-out of the telescopic (slip) joint (TJ)
- Stroke-out of the tensioners
- Maximum equivalent stresses in the riser must be ≤ yield
- Maximum equivalent stresses in the 36-in structural conductor casing must be ≤ yield
- Maximum bending moment in the wellhead must be less than its allowable based upon tension and pressure.
- Maximum bending moment in the structural conductor casing must be less than its allowable.
- Maximum unity checks, per API RP 2A, must be less than 1.

The riser is modeled in ABAQUS; ABAQUS is a general-purpose finite element program, which can model non-linearity of geometry, material properties, and spring definitions. ABAQUS includes the AQUA feature specifically designed for the analysis of beam-like structures installed underwater and subject to loading by water currents and wave action.

The Drift-Off and Drive-Off analysis employs the time domain capability of ABAQUS. The vessel offset (eg as shown in figure 2.4.6 and 2.4.7) is imposed as a function of time in the Drift-Off and Drive-Off analysis, which together with the current results in the inertial (mass) effects affecting riser response. The following are utilized in the analyses:

- For the Drift-Off and Drive-Off analysis, the vessel offset is a function of time. Note that wave frequency motions were not included in the model. However, separate analyses were performed to estimate the dynamic flex joint angles and vessel yaw at a given offset and heading.
- linear material stress-strain law,
- non-linear three-dimensional spring elements to model the tensioners,
- slider/contact elements to model the motion between the inner and outer barrel of the telescopic joint,
- non-linear springs to model the soil characteristics,
- beam elements to model all pipe sections.

The finite elements utilized were the ABAQUS PIPE31 three-dimensional beam element. This element accounts for internal and external hydrostatic pressure effects, using the HP option, which calculates the correct hoop stresses in the pipe due to fluid pressure, and then calculates the correct von Mises stress without any further post-processing. Furthermore, ABAQUS allows for pressure end loads to be modeled correctly, i.e. when there is a change in internal or external diameter of the riser.

Wire rope tensioners or direct acting tensioners are modeled as three-dimensional non-linear springs. The tensioners are assumed to be operating at a given stroke range, it is conservative for the Drive-Off and Drift-Off analysis to assume the smallest allowable stroke in the stroke range, thus leading to smaller watch circles.

During Drift-Off or Drive-Off, the tensioner springs initially respond according to their spring rate defined by the APV, accumulators, air volume, etc, until either a tensioner strokes out or the slip joint strokes out fully. The SPRINGA element was used to model the tensioners. After a tensioner strokes out, the tensioner responds, at a much higher spring rate/stiffness, essentially in a rigid manner. The flex joints were modeled in a similar manner using SPRING2 elements.

A “relatively” fine mesh was employed. the mesh was adjusted until the effective tension and stress distribution as predicted by ABAQUS was within 1% of that predicted by an independent program with the vessel located over the well (0% offset).

The finite element analysis first consists of pre-loading the riser with its distributed wet self weight, followed by internal and external hydrostatic pressurization. The vessel is then offset as a function of the input time trace. The RESTART and NLGEOM (non-linear geometry) options are utilized after each step to account for the riser configuration in the preceding step.

In addition:

- Riser contact modeling with the vessel sub-structure is not usually considered, however the top angle of the upper flex joint is monitored.
- At the start of the computer simulation, the appropriate top tension was applied which moves the TJ outer barrel up from its initial position. As the vessel moves in the lateral direction, the total displacement of the tensioners is equal to the initial stretch of the riser (upward motion of the slip ring when the top tension is applied) plus the values of tensioner stroke.
- The weight of the telescopic joint inner barrel, diverter housing and upper flex joint are assumed to be carried by the vessel.
- Soil support is usually assumed and modeled by equivalent soil springs, based upon soil data at the site provided and using API RP 2A.

For the Drift-Off/Drive-Off analysis, the riser stroke includes contributions from:

- Tide
- Heave (Function of heading).

i.e. $$T_{total} = Initial\ Stroke + T_{Offset}(t) + T_{Tide} < Stroke\text{-}Limit - 1.86 * T_{Heave}/2 \qquad (25)$$

The total stroke is defined as the available stroke plus the stroke due to offset of the vessel and due to tide. This total stroke must be less than the stroke limit minus the most probable heave.

The procedures to determine yellow and red alarms/watch circles are as follows:

- The time of disconnect is usually identified for each Drift-Off and Drive-Off condition (environment, mud weight, tension) as the time at which the first limiting criterion exceeds its corresponding allowable (maximum).
- The Red watch circle is then defined by subtracting off a specified time buffer from the point of disconnect.
- The Yellow watch circle is then defined by subtracting off a specified time buffer from the Red watch circle.

However, alternate criterion can also be used to determine the watch circles, **for instance**:

- FOR DRILLING: - The offset corresponding to the yellow alarm is assumed to be given, let's say 50-ft, for instance. The red alarm settings are selected to allow a maximum of a given time interval, let's say a 90-second buffer between the time that the vessel is at this offset and the time that disconnect sequence must initiate. It then takes an additional time interval, let's say 70-seconds from the beginning of EDS until the LMRP is free to lift-off the BOP, i.e.
    - Y – 50-ft Offset
    - Y-R – 90-seconds
    - R-Disconnect – 70-seconds

- FOR NON-DRILLING: - The rig may be assumed to be in perpetually in the yellow mode. The disconnect time may be assumed to occur when the rig reaches a given heading. The Red watch circle is then defined by providing a 70-second buffer between disconnect and this given heading.

Figure 3.1 shows and Table 3.1 the response characteristics for a given environment as a function of time. These figures are produced for a number of environments and drilling/non-drilling tensions.

| Time (secs) | Drive Off Heading (deg) | Significant Heave - S.A. (ft) -based on Heading | Conductor Casing VME Stress (ksi) | Total Lower Flex Joint Angle (deg) | Total Intermediate Flex Joint Angle (deg) | Total Upper Flex Joint Angle (deg) | TOTAL TENSIONER STROKE (ft) | ALLOWABLE TENSIONER STROKE (ft) |
|---|---|---|---|---|---|---|---|---|
| 0 | 15.00 | 1.57 | 3.52 | 0.78 | 0.28 | 1.59 | -21.99 | -46.93 |
| 5 | 15.38 | 1.57 | 3.52 | 0.78 | 0.28 | 1.62 | -21.99 | -46.93 |
| 25 | 16.80 | 1.59 | 3.52 | 0.78 | 0.27 | 1.87 | -22.02 | -46.91 |
| 50 | 18.51 | 1.61 | 3.57 | 0.81 | 0.28 | 2.22 | -22.08 | -46.89 |
| 75 | 20.41 | 1.64 | 5.24 | 1.50 | 0.29 | 2.67 | -23.09 | -46.86 |
| 100 | 22.77 | 1.68 | 6.90 | 2.05 | 0.29 | 3.23 | -23.17 | -46.82 |
| 125 | 25.88 | 1.75 | 9.27 | 2.66 | 0.30 | 3.91 | -25.17 | -46.75 |
| 150 | 30.03 | 1.87 | 12.31 | 3.28 | 0.30 | 4.66 | -28.18 | -46.63 |
| 175 | 35.49 | 2.09 | 16.13 | 3.85 | 0.30 | 5.46 | -32.18 | -46.41 |
| 200 | 42.54 | 2.52 | 20.91 | 4.33 | 0.33 | 6.21 | -37.22 | -45.98 |
| 225 | 51.47 | 3.34 | 26.90 | 4.64 | 0.32 | 7.03 | -43.31 | -45.16 |
| 230 | 53.50 | 3.58 | 28.21 | 4.70 | 0.33 | 7.19 | -45.28 | -44.92 |
| 235 | 55.63 | 3.85 | 29.65 | 4.74 | 0.33 | 7.35 | -47.28 | -44.65 |

*Table 3.1: Drive-Off Results 99% NX Winter Storm - 15-ppg 1327-kips*

**Figure 3.1: Drive-OFF ANALYSIS RESULTS - TOP TENSION = 1327-KIPS**
**(99% NX Winter Storm, Hs = 12.2-ft, Tp = 9.3-sec, γ = 1, Mud=15-ppg)**
**VESSEL**
**[CLIENT - SITE Connected Analyses in XXXX-ft Water Depth, X-deg Heading Initial Heading]**

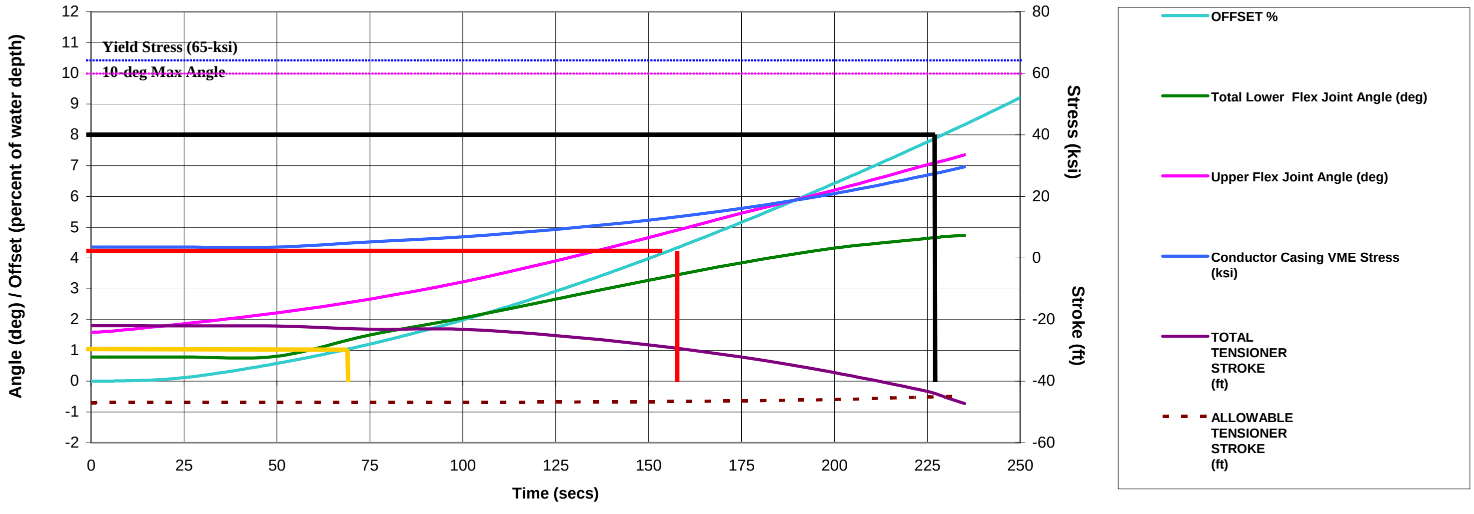

In addition Table 3.2 and 3.3 shows the watch circle/EDS times for a number of environments for drilling and NON-drilling conditions.

A number of conclusions and observations can be made. For instance, it is evident from table 3.2, for DRILLING that there are adequately defined watch circles for the 95% NX WS and the 99% NX WS for the Drift-Off and Drive-Off conditions. Moreover, it is apparent that there are no watch circles for the 1-yr WS DRILLING mode for the Drift-Off and Drive-Off conditions. Thus, it may be prudent to consider the 1-yr WS as a NON-DRILLING environment.

For NON-DRILLING, the vessel is in the yellow alarm mode perpetually and disconnect will occur prior to the vessel reaching a given heading (from an initial heading). A 70-second interval is used to define the red watch circle from this disconnect criterion. In this case the smallest watch circles are defined by Drive-Off; the 99% NX WS, 1-yr Loop, 1-yr WS and 5-yr WS red watch circles are 84-ft, 90-ft, 34-ft and 26-ft, respectively.

## 4.0 CONCLUDING REMARKS

A procedure has been developed to predict the vessel trajectory in a Drive-Off or Drift-Off event based upon an environment. The results from measurements of the vessel tests (*e.g.* the maneuvering tests and sea trial tests) are very useful for determining/collaborating the important hydrodynamic derivatives of the vessels to build a good simulation model for the vessel trajectories. The vessel's hydrodynamic derivatives, however, may also be estimated using theoretical or numerical approximations when the test data is not available or insufficient. A combined use of the test data and theoretical /numerical approximation has shown to be a prudent approach.

The vessel trajectory can be used to determine the point of disconnect and red, yellow and green watch circles based upon the EDS times. Thus, the integrity of the riser is not compromised in such an event.

## *Table 3.2: Watch Circle Definition for Drilling*

| CASES | | | | | | | | | | | | Drilling Riser Response at Disconnect Time | | | | | | |
|---|---|---|---|---|---|---|---|---|---|---|---|---|---|---|---|---|---|---|
| Weather | DRILLING | Mud (ppg) | Top Tension (kips) | YELLOW WATCH CIRCLE FOR EDS (sec) Time at which 50-ft Offset is reached | RED WATCH CIRCLE FOR EDS (sec) | RED WATCH CIRCLE FOR EDS (ft) | RED WATCH CIRCLE FOR EDS (% Offset) | DISCONNECT TIME (sec) | DISCONNECT OFFSET (ft) | DISCONNECT (% Offset) | Have the Tensioners Stroked-Out ? | Upper Flex Joint Angle (deg) | Lower Flex Joint Angle (deg) | Intermediate Flex Joint Angle (deg) | VME Stress 36-in Casing (ksi) | API Unity Check | API Max Unity Check |
| | | | | | | | | | | | | | | | | | |
| 95% NX | DRIFT-OFF | 8.56 | 632.0 | 93 | 183 | 187 | 2.55 | 253 | 347 | 4.75 | NO | 4.39 | 2.41 | 0.70 | 11.28 | 0.286 | 0.215 |
| 95% NX | DRIFT-OFF | 12 | 912.0 | 93 | 183 | 187 | 2.55 | 253 | 347 | 4.75 | NO | 3.71 | 3.91 | 0.43 | 13.32 | 0.330 | 0.248 |
| 95% NX | DRIFT-OFF | 15 | 1327.0 | 93 | 183 | 187 | 2.55 | 253 | 347 | 4.75 | NO | 3.32 | 3.93 | 0.27 | 16.94 | 0.404 | 0.304 |
| | | | | | | | | | | | | | | | | | |
| 99% NX | DRIFT-OFF | 8.56 | 709.8 | 71 | 161 | 246 | 3.36 | 231 | 483 | 6.60 | NO | 7.60 | 2.48 | 0.79 | 14.32 | 0.352 | 0.264 |
| 99% NX | DRIFT-OFF | 12 | ▨ | ▨ | ▨ | ▨ | ▨ | ▨ | ▨ | ▨ | ▨ | ▨ | ▨ | ▨ | ▨ | ▨ | ▨ |
| 99% NX | DRIFT-OFF | 15 | 1330.8 | 71 | 161 | 246 | 3.36 | 231 | 483 | 6.60 | NO | 5.99 | 4.38 | 0.32 | 20.92 | 0.494 | 0.372 |
| | | | | | | | | | | | | | | | | | |
| ** 1 yr WS | DRIFT-OFF | 8.56 | 907.7 | 52 | 142 | 346 | 4.73 | 212 | 698 | 9.55 | YES | > 10 | 1.14 | 1.33 | 35.28 | 0.702 | 0.528 |
| ** 1 yr WS | DRIFT-OFF | 12 | ▨ | ▨ | ▨ | ▨ | ▨ | ▨ | ▨ | ▨ | ▨ | ▨ | ▨ | ▨ | ▨ | ▨ | ▨ |
| ** 1 yr WS | DRIFT-OFF | 15 | 1338.8 | 52 | 142 | 346 | 4.73 | 212 | 698 | 9.55 | YES | > 10 | 2.54 | 0.85 | 40.75 | 0.804 | 0.605 |
| | | | | | | | | | | | | | | | | | |
| 95% NX | DRIVE-OFF | 8.56 | 632.0 | 64 | 154 | 215 | 2.94 | 224 | 397 | 5.42 | NO | 5.22 | 2.63 | 0.73 | 12.57 | 0.305 | 0.230 |
| 95% NX | DRIVE-OFF | 12 | 912.0 | 64 | 154 | 215 | 2.94 | 224 | 397 | 5.42 | NO | 5.01 | 4.64 | 0.44 | 15.10 | 0.357 | 0.268 |
| 95% NX | DRIVE-OFF | 15 | 1327.0 | 64 | 154 | 215 | 2.94 | 224 | 397 | 5.42 | NO | 3.91 | 4.22 | 0.27 | 19.64 | 0.446 | 0.335 |
| | | | | | | | | | | | | | | | | | |
| 99% NX | DRIVE-OFF | 8.56 | 709.8 | 55 | 145 | 275 | 3.76 | 215 | 528 | 7.22 | NO | 8.53 | 2.67 | 0.80 | 16.14 | 0.377 | 0.284 |
| 99% NX | DRIVE-OFF | 12 | ▨ | ▨ | ▨ | ▨ | ▨ | ▨ | ▨ | ▨ | ▨ | ▨ | ▨ | ▨ | ▨ | ▨ | ▨ |
| 99% NX | DRIVE-OFF | 15 | 1330.8 | 55 | 145 | 275 | 3.76 | 215 | 528 | 7.22 | NO | 6.70 | 4.51 | 0.32 | 24.56 | 0.543 | 0.408 |
| | | | | | | | | | | | | | | | | | |
| ** 1 yr WS | DRIVE-OFF | 8.56 | 907.7 | 44 | 134 | 372 | 5.09 | 204 | 744 | 10.17 | YES | > 10 | 0.86 | 1.18 | 42.04 | 0.855 | 0.643 |
| ** 1 yr WS | DRIVE-OFF | 12 | ▨ | ▨ | ▨ | ▨ | ▨ | ▨ | ▨ | ▨ | ▨ | ▨ | ▨ | ▨ | ▨ | ▨ | ▨ |
| ** 1 yr WS | DRIVE-OFF | 15 | 1338.8 | 44 | 134 | 372 | 5.09 | 204 | 744 | 10.17 | YES | > 10 | 1.91 | 0.92 | 47.20 | 0.952 | 0.716 |

** A limit has been exceeded before the defined disconnect offset/time. Thus, the watch circles for theses cases are being redefined below :

| | | | | | | | | | | | | Drilling Riser Response at Disconnect Time | | | | | | |
|---|---|---|---|---|---|---|---|---|---|---|---|---|---|---|---|---|---|---|
| Weather | DRILLING | Mud (ppg) | Top Tension (kips) | YELLOW WATCH CIRCLE FOR EDS (sec) | YELLOW WATCH CIRCLE FOR EDS (ft) | RED WATCH CIRCLE FOR EDS (sec) | RED WATCH CIRCLE FOR EDS (ft) | RED WATCH CIRCLE FOR EDS (% Offset) | DISCONNECT TIME (sec) | DISCONNECT OFFSET (ft) | DISCONNECT (% Offset) | Have the Tensioners Stroked-Out ? | Upper Flex Joint Angle (deg) | Lower Flex Joint Angle (deg) | Intermediate Flex Joint Angle (deg) | VME Stress 36-in Casing (ksi) | API Unity Check | API Max Unity Check |
| ** 1 yr WS | DRIFT-OFF | 8.56 | 907.7 | 5 | 7.3 | 95 | 213 | 2.91 | 165 | 529 | 7.23 | NO | 10.00 | 1.82 | 0.64 | 14.11 | 0.331 | 0.249 |
| ** 1 yr WS | DRIFT-OFF | 12 | ▨ | ▨ | ▨ | ▨ | ▨ | ▨ | ▨ | ▨ | ▨ | ▨ | ▨ | ▨ | ▨ | ▨ | ▨ | ▨ |
| ** 1 yr WS | DRIFT-OFF | 15 | 1338.8 | 30 | 16.4 | 120 | 252 | 3.44 | 190 | 580 | 7.93 | YES | 10.00 | 4.23 | 0.39 | 23.39 | 0.521 | 0.392 |
| | | | | | | | | | | | | | | | | | | |
| ** 1 yr WS | DRIVE-OFF | 8.56 | 907.7 | 0 | 0 | 75 | 204 | 2.79 | 145 | 525 | 7.18 | NO | 10.00 | 1.69 | 0.62 | 12.77 | 0.302 | 0.227 |
| ** 1 yr WS | DRIVE-OFF | 12 | ▨ | ▨ | ▨ | ▨ | ▨ | ▨ | ▨ | ▨ | ▨ | ▨ | ▨ | ▨ | ▨ | ▨ | ▨ | ▨ |
| ** 1 yr WS | DRIVE-OFF | 15 | 1338.8 | 10 | 1.83 | 100 | 224 | 3.05 | 170 | 551 | 7.53 | YES | 9.80 | 4.07 | 0.39 | 21.22 | 0.477 | 0.358 |

## *Table 3.3: Watch Circle Definition for NON-Drilling*

| CASES | | | | | | | | | | NON-Drilling Riser Response at Disconnect Time | | | | | | |
|---|---|---|---|---|---|---|---|---|---|---|---|---|---|---|---|---|
| Weather | NON-DRILLING | Mud (ppg) | Top Tension (kips) | RED WATCH CIRCLE FOR EDS (sec) | RED WATCH CIRCLE FOR EDS (ft) | RED WATCH CIRCLE FOR EDS (% Offset) | DISCONNECT TIME (30-deg Yaw Angle) (sec) | DISCONNECT OFFSET (ft) | DISCONNECT (% Offset) | Have the Tensioners Stroked-Out ? | Upper Flex Joint Angle (deg) | Lower Flex Joint Angle (deg) | Intermediate Flex Joint Angle (deg) | VME Stress 36-in Casing (ksi) | API Unity Check | API Max Unity Check |
| 99% NX | DRIFT-OFF | 8.56 | 709.8 | 126 | 150 | 2.05 | 196 | 357 | 4.88 | NO | 6.57 | 2.12 | 0.73 | 11.69 | 0.285 | 0.214 |
| 99% NX | DRIFT-OFF | 12 | 912.0 | 126 | 150 | 2.05 | 196 | 357 | 4.88 | NO | 5.83 | 3.74 | 0.51 | 12.68 | 0.306 | 0.230 |
| 99% NX | DRIFT-OFF | 15 | 1327.0 | 126 | 150 | 2.05 | 196 | 357 | 4.88 | NO | 5.22 | 3.92 | 0.30 | 16.36 | 0.378 | 0.284 |
| 1 yr Loop NX | DRIFT-OFF | 8.56 | 632.0 | 193 | 138 | 1.89 | 263 | 247 | 3.38 | NO | 0.53 | 1.99 | 0.51 | 10.22 | 0.256 | 0.193 |
| 1 yr Loop NX | DRIFT-OFF | 12 | 912 | 193 | 138 | 1.89 | 263 | 247 | 3.38 | NO | 0.61 | 3.25 | 0.35 | 11.51 | 0.282 | 0.212 |
| 1 yr Loop NX | DRIFT-OFF | 15 | 1327.0 | 193 | 138 | 1.89 | 263 | 247 | 3.38 | NO | 0.77 | 3.12 | 0.25 | 13.87 | 0.327 | 0.246 |
| 1 yr WS | DRIFT-OFF | 8.56 | 709.8 | 68 | 83 | 1.14 | 138 | 328 | 4.48 | NO | 9.00 | 1.71 | 0.88 | 9.10 | 0.230 | 0.173 |
| 1 yr WS | DRIFT-OFF | 12 | ▨ | ▨ | ▨ | ▨ | ▨ | ▨ | ▨ | ▨ | ▨ | ▨ | ▨ | ▨ | ▨ | ▨ |
| 1 yr WS | DRIFT-OFF | 15 | 1327.0 | 68 | 83 | 1.14 | 138 | 328 | 4.48 | NO | 7.41 | 3.34 | 0.37 | 12.17 | 0.291 | 0.218 |
| 5 yr WS | DRIFT-OFF | 8.56 | 709.8 | 57 | 67 | 0.92 | 127 | 321 | 4.39 | NO | 10.00 | 1.62 | 0.87 | 8.68 | 0.221 | 0.276 |
| 5 yr WS | DRIFT-OFF | 12 | ▨ | ▨ | ▨ | ▨ | ▨ | ▨ | ▨ | ▨ | ▨ | ▨ | ▨ | ▨ | ▨ | ▨ |
| 5 yr WS | DRIFT-OFF | 15 | 1327.0 | 57 | 67 | 0.92 | 127 | 321 | 4.39 | NO | 8.42 | 3.26 | 0.37 | 11.47 | 0.166 | 0.207 |
| 99% NX | DRIVE-OFF | 8.56 | 709.8 | 73 | 84 | 1.15 | 143 | 269 | 3.67 | NO | 5.61 | 1.35 | 0.70 | 8.90 | 0.226 | 0.170 |
| 99% NX | DRIVE-OFF | 12 | 912.0 | 73 | 84 | 1.15 | 143 | 269 | 3.67 | NO | 5.02 | 2.43 | 0.50 | 9.42 | 0.238 | 0.179 |
| 99% NX | DRIVE-OFF | 15 | 1327.0 | 73 | 84 | 1.15 | 143 | 269 | 3.67 | NO | 4.51 | 2.54 | 0.30 | 11.66 | 0.280 | 0.211 |
| 1 yr Loop NX | DRIVE-OFF | 8.56 | 632.0 | 106 | 90 | 1.23 | 176 | 195 | 2.66 | NO | 0.07 | 1.57 | 0.49 | 8.58 | 0.221 | 0.166 |
| 1 yr Loop NX | DRIVE-OFF | 12 | 912 | 106 | 90 | 1.23 | 176 | 195 | 2.66 | NO | 0.26 | 2.59 | 0.34 | 9.32 | 0.236 | 0.177 |
| 1 yr Loop NX | DRIVE-OFF | 15 | 1327.0 | 106 | 90 | 1.23 | 176 | 195 | 2.66 | NO | 0.45 | 2.55 | 0.25 | 10.77 | 0.262 | 0.197 |
| 1 yr WS | DRIVE-OFF | 8.56 | 709.8 | 37 | 34 | 0.47 | 107 | 252 | 3.44 | NO | 8.06 | 1.37 | 0.83 | 7.38 | 0.185 | 0.139 |
| 1 yr WS | DRIVE-OFF | 12 | ▨ | ▨ | ▨ | ▨ | ▨ | ▨ | ▨ | ▨ | ▨ | ▨ | ▨ | ▨ | ▨ | ▨ |
| 1 yr WS | DRIVE-OFF | 15 | 1327.0 | 37 | 34 | 0.47 | 107 | 252 | 3.44 | NO | 6.70 | 2.78 | 0.36 | 9.19 | 0.215 | 0.161 |
| 5 yr WS | DRIVE-OFF | 8.56 | 709.8 | 31 | 26 | 0.35 | 101 | 253 | 3.46 | NO | 8.81 | 1.25 | 0.84 | 6.86 | 0.181 | 0.136 |
| 5 yr WS | DRIVE-OFF | 12 | ▨ | ▨ | ▨ | ▨ | ▨ | ▨ | ▨ | ▨ | ▨ | ▨ | ▨ | ▨ | ▨ | ▨ |
| 5 yr WS | DRIVE-OFF | 15 | 1327.0 | 31 | 26 | 0.35 | 101 | 253 | 3.46 | NO | 7.45 | 2.64 | 0.37 | 8.27 | 0.208 | 0.156 |